

**CARBON 72: pp. 425-428. (2014)**  
**Intercalation and coordination of copper (II) 2,2'-bipyridine complexes into graphite oxide**

Tamás Szabó <sup>a,\*</sup>, Terézia Szabó-Plánka <sup>a</sup>, Dominika Jónás <sup>a</sup>, Nóra Veronika Nagy <sup>b</sup>,  
Antal Rockenbauer <sup>b</sup>, Imre Dékány <sup>a</sup>

<sup>a</sup> *Department of Physical Chemistry and Materials Science, University of Szeged, Aradi vértanúk tere 1, H-6720 Szeged, Hungary*

<sup>b</sup> *Institute of Structural Chemistry, Chemical Research Center, Hungarian Academy of Sciences, Pusztaszeri út 59-67, H-1025 Budapest, Hungary*

**Abstract**

Copper-intercalated graphite oxides (GO) were prepared by adding complex solutions of cupric ions and 2,2'-bipyridine (L) ligands to exfoliated GO suspension at pH = 7. High adsorption capacity (>140 mg Cu/g GO) was found for adsorption from equimolar solution of Cu<sup>2+</sup> and L, while the excess of ligand results in progressively decreasing adsorbed amounts. Electron spin resonance spectra revealed two principal adsorption mechanisms: the [CuL<sub>3</sub>]<sup>2+</sup> complex undergoes ion exchange adsorption, while [CuL]<sup>2+</sup> and [CuL<sub>2</sub>]<sup>2+</sup> bind to graphene oxide by coordination.

---

Graphene-based nanocomposites of transition metals, metal oxides or metal-organic frameworks have stimulated intense research over the past few years because of promising applications as high-surface-area supported catalysts, supercapacitors or biosensors [1,2]. The solution-based construction methods of these composites are very versatile but, in general, they rely on the same principle: adsorption of metal precursors on exfoliated graphite oxide (GO) in aqueous dispersion followed by transformation to graphene-supported metal/metal oxide nanoparticles. Crucial to the improvement of this synthetic route, together with potential use for removal of toxic inorganic contaminants from water, is the understanding of the adsorption mechanism of transitional metal ions and their complexes on GO. Quantitative characterization has first been performed for the

---

\*Corresponding author. Tel.: +36-62-544211; fax: +36-62-544042.  
E-mail address: sztamas@chem.u-szeged.hu (Tamás Szabó).

adsorption of  $\text{Cu}^{2+}$  by Yang et al. [3]. They found a high adsorption capacity of ca. 47 mg/g at pH = 5. In line with other reports [1,4,5], this strongly suggested for the coordination of GO's oxygen functionalities to the cupric ions, although ion exchange could not be ruled out [6]. In order to obtain direct molecular-level information on the binding mode of copper, we studied the adsorption of Cu(II) 2,2'-bipyridyl complexes of different compositions on GO by electron paramagnetic resonance (EPR) spectroscopy, supplementing the adsorption and X-ray diffraction (XRD) data.

Adsorption of copper species was studied in neutral saline solution (pH=7, 20 mM  $\text{NaNO}_3$ ), where GO has sufficiently high surface charge to undergo exfoliation and produce single- and few-layer graphene oxide [7] (experimental details are found as Supplementary Information). Neutral 2,2'-bipyridine molecule was chosen as ligand (L) and added to the  $\text{Cu}(\text{NO}_3)_2$  solution in order to avoid precipitation of copper at pH = 7. Isotherms were constructed at different total analytical concentrations of Cu ( $T_{\text{Cu}}$ ) and the ligand ( $T_{\text{L}}$ ) to examine adsorption from solution in which one of the three homoleptic complex species  $\text{CuL}_n^{2+}$  ( $n=1,2,3$ : monocomplex, biscomplex or triscomplex, respectively) is dominant. To this aim, the distribution diagrams of copper(II)/L systems of various  $T_{\text{Cu}}$  at pH = 7 (displayed in Fig. 1 along with the chemical structures of the complex species) were calculated by an EPR software [8] using experimentally determined complex stability constants [9].

Dominant species ( $\geq 90\%$ ) in the starting complex solutions are  $\text{CuL}^{2+}$  for equimolar mixtures of  $\text{Cu}^{2+}/\text{L}$ ,  $\text{CuL}_2^{2+}$  for double ligand excess, and  $\text{CuL}_3^{2+}$  for  $T_{\text{Cu}}:T_{\text{L}} = 1:5$ .<sup>†</sup> Fig. 2 shows the adsorption isotherms of copper complexes on GO at the above three metal-to-ligand ratios. They are H-type isotherms characterized by quantitative adsorption up to a certain loading. The steeply increasing adsorbed amounts in this region indicate strong interaction between the solute and adsorbent surface. Rapid coagulation of the suspension upon addition of the complex solutions also inferred high affinity of copper species to GO. At  $T_{\text{Cu}}:T_{\text{L}} = 1:5$ , quantitative adsorption roughly coincided with the maximum amount of adsorbed Cu (0.41 mmol/g = 26 mg/g). At a lower ligand excess of  $T_{\text{Cu}}:T_{\text{L}} = 1:2$ , greater initial concentrations yielded a non-linear increase of adsorbed

---

<sup>†</sup> It is noted, though, that the contribution of  $[\text{Cu}_2\text{L}_2(\text{OH})_2]^{2+}$  in concentrated solutions at  $T_{\text{Cu}}:T_{\text{L}} = 1:1$ , and  $\text{CuL}_2^{2+}$  in dilute solutions at  $T_{\text{Cu}}:T_{\text{L}} = 1:5$  becomes more pronounced at the expense of  $\text{CuL}^{2+}$  and  $\text{CuL}_3^{2+}$ ; see Fig 1.

amount, tending towards an adsorption capacity of 1.55 mmol/g (99 mg/g). Finally, in equimolar solutions of  $\text{Cu}(\text{NO}_3)_2$  and L, a continuous increase in the amount of adsorbed copper was found without reaching a plateau in the studied range; the highest loading was 2.18 mmol/g or 139 mg/g. These high capacities considerably exceed those obtained for  $\text{Cu}^{2+}$  adsorption on GO at pH=5 (47 mg/g, [3]) or on activated carbon based sorbents (typically 5-20 mg/g), and they are also higher than the maximum amount of exchangeable divalent cations on GO ( $\text{CEC}/2 = 0.175 \text{ mmol Me}^{2+}/\text{g GO}$  at pH = 7 and 20 mM ionic strength, [7]). Therefore, it is clear that mechanisms other than ion-exchange (most likely surface complexation) must operate upon the sorption of  $\text{CuL}_n$  complexes. Since all of these species have the same charge of +2, a purely ion-exchange based binding mechanism would give rise to the same adsorption capacity (i.e.  $\text{CEC}/2$ ) because the surface charge of GO is constant at constant pH and ionic strength.

The Cu-loaded GO samples used in the adsorption experiments exhibited broad, blurred EPR spectra, which are difficult to analyze. To reduce linewidth, adsorption at lower  $T_{\text{Cu}}$  ( $\leq 0.04 \text{ mM}$ ) and  $T_{\text{L}}$  was carried out. The low g values and resolved superhyperfine pattern by the ligand N donors for the spectra of the latter samples (Fig. 3) support that L is coordinated to  $\text{Cu}^{2+}$  adsorbed on GO. At low concentration of the complex solutions, the EPR spectra of the samples obtained at  $T_{\text{Cu}} < T_{\text{L}}$  (where  $\text{CuL}_2^{2+}$  and  $\text{CuL}_3^{2+}$  predominate in the solution) are closely similar to those gained at  $T_{\text{Cu}} = T_{\text{L}}$ , when only  $\text{CuL}^{2+}$  can be adsorbed. This shows that the adsorption of the monocomplex, which has two strong equatorial and two weak axial coordination sites for the O donor groups of GO (carboxylate, phenolate and tertiary OH), is particularly favoured.  $\text{CuL}_2^{2+}$  has merely two weak axial sites for GO (if it is flattened between the adjacent graphene layers), while  $\text{CuL}_3^{2+}$  can be adsorbed only by ion-exchange mechanism. At  $T_{\text{Cu}} = T_{\text{L}}$ , the dominating monocomplex is readily chemisorbed, while at excess L, GO either has to replace one or two molecules of L from the complexes present in the solution, or they can only be bound electrostatically at ion exchange sites (carboxylate and phenolate but not to uncharged tertiary OH). This explains why the maximum adsorbed amount of  $\text{Cu}^{2+}$  decreases with increasing excess of L (Fig. 2). The experimental spectra

are the superpositions of two component curves, suggesting two different coordination environments around  $\text{Cu}^{2+}$  bound to GO. For both of them, the g values are lower than for the monocomplex in the solution, indicating stronger ligand field formed by the coordination to GO.

X-ray diffractograms of air-dry Cu-modified graphite oxides prepared at different metal-to-ligand ratios containing low and high amounts of complexes are compared in Fig.4. At low loadings (ca. 0.4 mmol/g), two peaks appear near diffraction angles of  $\sim 10^\circ$  and  $\sim 20^\circ$ , characteristic of (001) and (002) lattice planes. Basal spacings show subtle changes from 0.84 to 0.88 nm with decreasing  $T_{\text{Cu}}:T_{\text{L}}$ . These distances are larger than the d-spacing of air-dry GO (typically 0.7 nm), which suggests that the complexes intercalated into graphite oxide. For  $T_{\text{Cu}}:T_{\text{L}}$  of 1:1 and 1:2 at high loadings, the reflections are shifted towards lower angles, which implies that larger amounts of complexes are accommodated between graphene oxide sheets due to random interstratification. At 1:5 metal-to-ligand ratio, markedly different diffractograms appear at the same loading of ca. 0.4 mmol/g. Besides the aforementioned double-peak pattern of the sample prepared from a complex solution of  $T_{\text{Cu}} = 0.8$  mM, a higher total Cu concentration of 4 mM gave rise to a peak, together with its second order reflection, which relate to a 1.24 nm basal spacing. This can be explained by the presence of two different phases in this sample: one that contains nearly planar  $\text{CuL}_2^{2+}$  or  $\text{CuL}_2^{2+}$  (ligands aligning parallel to the GO sheet), and the other stuffed with much larger  $\text{CuL}_3^{2+}$ . At low initial concentration, copper is present in the starting solution as  $\text{CuL}_2^{2+}$  and  $\text{CuL}_3^{2+}$ . From this solution, the planar biscomplex is preferentially adsorbed, leading to a lower interlayer expansion. However, at  $T_{\text{Cu}} = 4$  mM, the triscomplex is dominant in the starting solution, and this is adsorbed at the expense of  $\text{CuL}_2^{2+}$ , while the total adsorbed amount remains similar to that at  $T_{\text{Cu}} = 0.8$  mM.

Overall, high quantities of Cu(II)-bipyridine complexes intercalate into graphite oxide without hydrolysis and concomitant precipitation of copper at pH = 7. The dominant binding modes (ion-exchange or coordination) as well as the structure and composition of the intercalation complexes highly depend on the metal-to-ligand ratio. Since the adsorbed metal ions constitute different

nucleation sites for nanoparticle growth, these results are of especial importance for controlled synthesis methods of chemically derived metal/graphene composite materials.

**Acknowledgements.** Tamás Szabó acknowledges support from the Magyary Zoltán postdoctoral fellowship funded by the EEA and Norway Grants. The Project named “TÁMOP-4.2.2.A-11/1/KONV-2012-0047” is supported by the EU and the European Regional Development Fund.

## **Appendix A. Supplementary data**

Supplementary data associated with this Letter can be found in the online version, at doi:XXXX

## **References**

- [1] Petit C, Burrell J, Bandosz TJ. The synthesis and characterization of copper-based metal-organic framework/graphite oxide composites. *Carbon* 2011; 49: 563-72.
- [2] Matsuo Y, Hatase K, Sugie Y. Preparation and characterization of poly(vinyl alcohol)- and Cu(OH)<sub>2</sub>-poly(vinyl alcohol)-intercalated graphite oxides. *Chem Mater* 1998; 10: 2266-9.
- [3] Yang ST, Chang Y, Wang H, Liu G, Chen S, Wang Y, et al. Folding/aggregation of graphene oxide and its application in Cu<sup>2+</sup> removal. *J Colloid Interface Sci* 2010; 351: 122-7.
- [4] Ren H, Wang C, Zhang J, Zhou X, Xu D, Zheng J, et al. DNA cleavage system of nanosized graphene oxide sheets and copper ions. *ACS Nano* 2010; 4: 7169-74.
- [5] Sitko R, Turek E, Zawisza B, Malicka E, Talik E, Heimann J, et al. Adsorption of divalent metal ions from aqueous solutions using graphene oxide. *Dalton Trans* 2013; 42: 5682-9.
- [6] Gotoh K, Kinumoto T, Fujii E, Yamamoto A, Hashimoto H, Ohkubo T, et al. Exfoliated graphene sheets decorated with metal/metal oxide nanoparticles: simple preparation from cation exchanged graphite oxide. *Carbon* 2011; 49: 1118-25.
- [7] Szabó T, Tombácz E, Illés E, Dékány I. Enhanced acidity and pH-dependent surface charge characterization of successively oxidized graphite oxides. *Carbon* 2006; 44: 537-45.

[8] Rockenbauer A, Korecz L. Automatic computer simulations of ESR spectra. *Appl Magn Reson* 1996; 10: 29-43.

[9] Fabian I. Hydrolytic reactions of copper(II) bipyridine complexes. *Inorg Chem* 1989;28:3805-7.

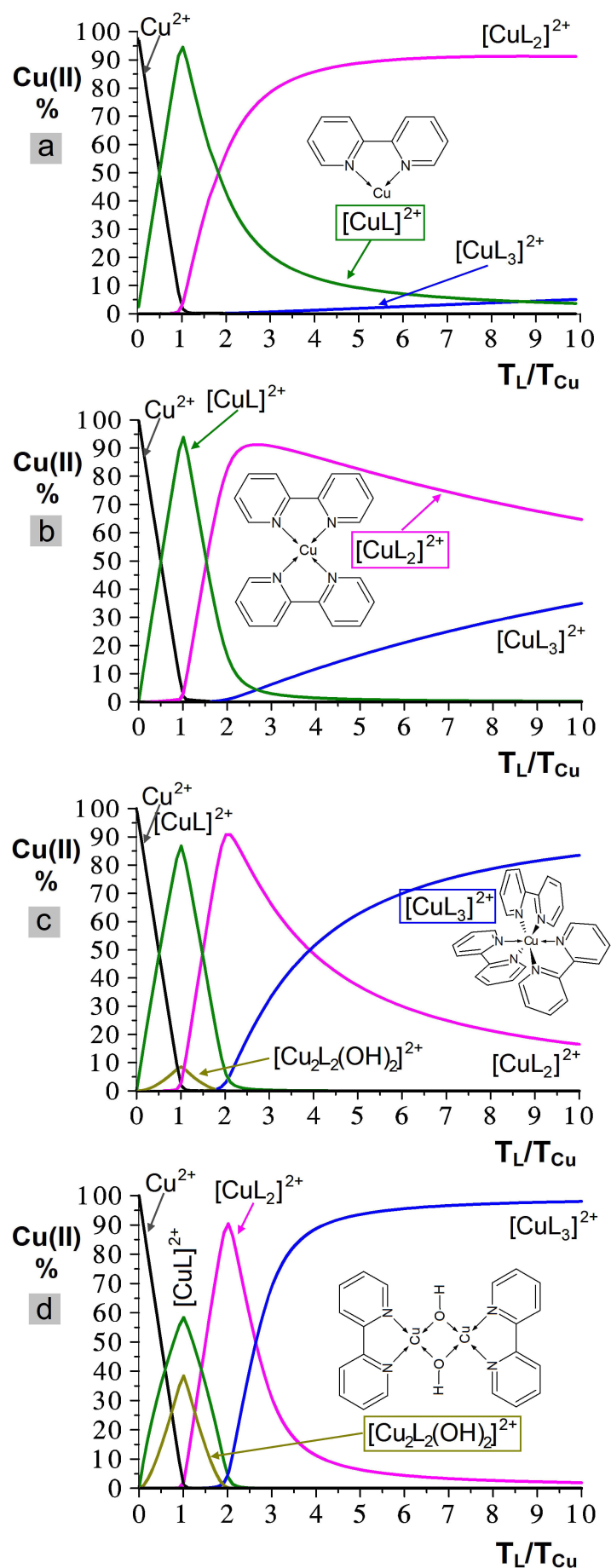


**Fig. 1** – Distribution curves of Cu(II)-2,2'-bipyridine complexes at  $T_{Cu} = 0.004$  mM (a), 0.04 mM (b), 0.4 mM (c), and 4 mM (d), pH = 7, including chemical structures of enframed complex species.

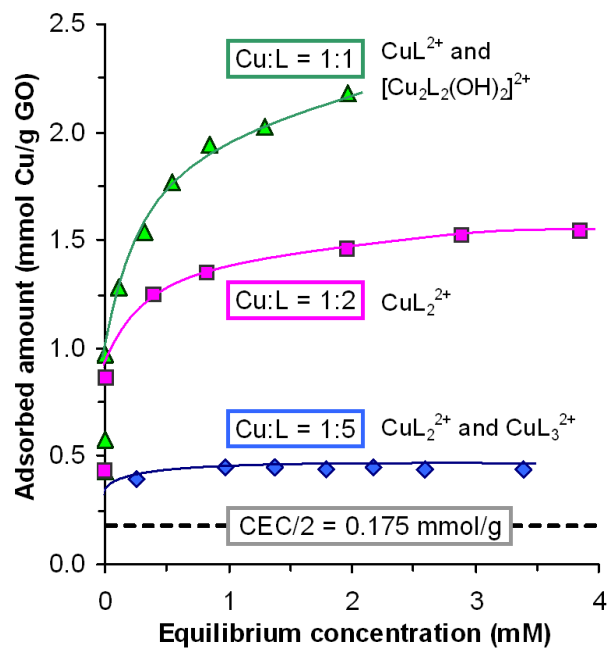


**Fig. 2** – Adsorption isotherms of copper(II)-bipyridine complexes on graphite oxide at different metal-to-ligand ratios (pH = 7, I = 20 mM).



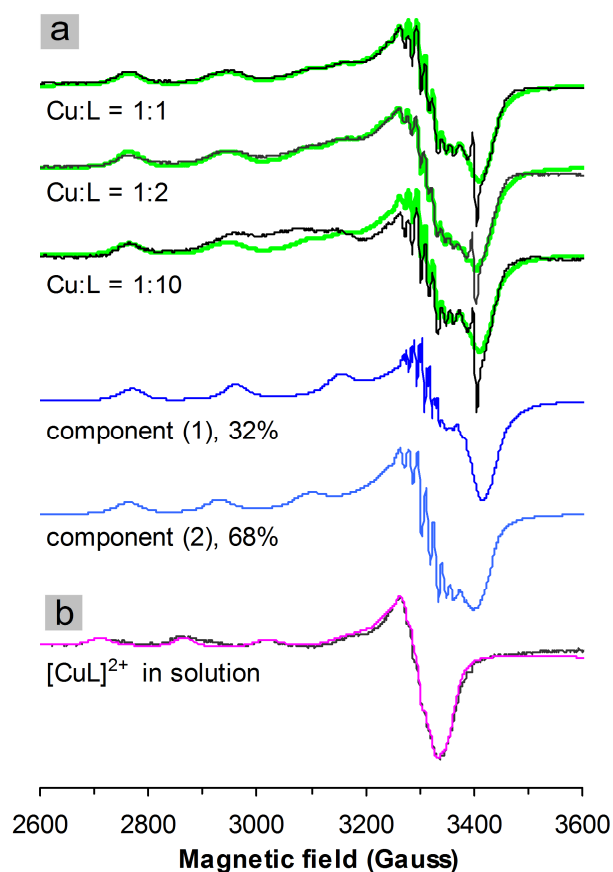


**Fig. 3** – EPR spectra of  $\text{CuL}_n^{2+}$  complexes (a) adsorbed on GO at  $T_{\text{Cu}}=T_{\text{L}}=0.016$  mM;  $T_{\text{Cu}}=0.02$  mM,  $T_{\text{L}}=0.04$  mM;  $T_{\text{Cu}}=0.04$  mM,  $T_{\text{L}}=0.4$  mM from top to bottom. Black: experimental, light green: calculated as superpositions of two component curves, blue: the component spectra with  $g_{xx}=2.050$ ,  $g_{yy}=2.034$ ,  $g_{zz}=2.225$ ,  $A_{xx}=14.3$  G,  $A_{yy}=17$  G,  $A_{zz}=187$  G for the minor, while with  $g_{xx}=2.069$ ,  $g_{yy}=2.030$ ,  $g_{zz}=2.258$ ,  $A_{xx}=34$  G,  $A_{yy}=23$  G,  $A_{zz}=169$  G for the major species. (b) in solution at  $T_{\text{Cu}}=T_{\text{L}}=1$  mM, pH=7; black: experimental, magenta: calculated with  $g_{xx}=g_{yy}=2.060$ ,  $g_{zz}=2.310$ ,  $A_{xx}=A_{yy}=9$  G,  $A_{zz}=150.5$  G.

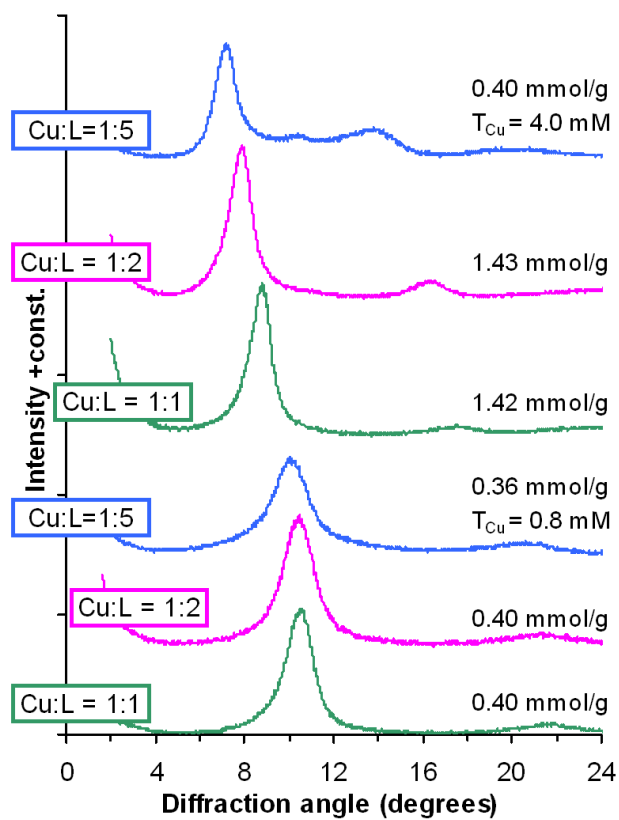


**Fig. 4** – XRD patterns of  $CuL_n$ -loaded graphite oxides at different metal-to-ligand ratios at lower (on the bottom) and higher (on the top) adsorbed amounts.